

## Dehydrogenation characteristic of $Zr_{1-x}M_xCo$ ( $M=Hf, Sc$ ) alloy

TAN Gong-li(谭功理), LIU Xiao-peng(刘晓鹏), JIANG Li-jun(蒋利军),  
WANG Shu-mao(王树茂), LI Zhi-nian(李志念), LI Hua-ling(李华玲)

General Research Institute for Nonferrous Metals, Beijing 100088, China

Received 15 July 2007; accepted 10 September 2007

**Abstract:** The intermetallic compound  $Zr_{1-x}Hf_xCo$  and  $Zr_{1-x}Sc_xCo$  ( $x=0, 0.1, 0.2, 0.3$ ) were prepared and their suitability for hydrogen storage was investigated. The alloys show single cubic phase identical with  $ZrCo$  by X-ray diffraction. Pressure-composition-temperature(PCT) measurement results show that the equilibrium dehydrogenation pressure of  $Zr_{1-x}Hf_xCo$  alloy increases obviously with increasing Hf content while it changes little with increasing Sc content for  $Zr_{1-x}Sc_xCo$  alloy. The dehydrogenation temperatures for supplying 100 kPa hydrogen are about 673, 627, and 650 K for  $ZrCo$ ,  $Zr_{0.7}Hf_{0.3}Co$  and  $Zr_{0.7}Sc_{0.3}Co$  alloy, respectively. Thermodynamics calculation results indicate that dehydrogenation  $\Delta H$  for  $Zr_{1-x}Hf_xCo$  alloy decreases with increasing Hf content but increases with increasing Sc content for  $Zr_{1-x}Sc_xCo$  alloy, which are coincident with their dehydrogenation property. The maximal hydrogen storage capacity of both  $Zr_{1-x}Hf_xCo$  and  $Zr_{1-x}Sc_xCo$  alloy at room temperature are high enough.

**Key words:** hydrogen storage alloy;  $ZrCo$ ;  $Zr_{1-x}Hf_xCo$ ;  $Zr_{1-x}Sc_xCo$ ; intermetallic compound

## 1 Introduction

Alloys and compounds having equilibrium absorption pressure less than 1 Pa at room temperature have large application in hydrogen isotope recovery and storage. Low equilibrium pressure is still preferable if the compound releases hydrogen isotope under high pressure at a moderate temperature because the penetration of tritium is more difficult.

Though the hydrogen storage capacity of metals such as Zr and Ti are high and their equilibrium absorption pressures are very low, their hydrides are too stable to be effectively utilized for isotopes release and separation application. The isotherm of intermetallic compound  $ZrCo-H$  was found to have advantageous features as a hydride media for recovery, storage and supply of hydrogen isotopes[1-2]. Typically,  $ZrCo$  alloy absorbs hydrogen isotopes down to 0.01 Pa at room temperature, and is elevated to approximately 673 K for desorbing hydrogen at surrounding atmospheric pressure. Because of this,  $ZrCo$  alloy has been selected as a potentially substituted getter material for uranium by the international thermonuclear experimental reactors(ITER) team[3-4]. However, there are problems that need to be dealt with, e.g. liable to be poisoning by impurity gases

such as  $H_2O$ ,  $O_2$  and  $CO_2$ , hydrogen-induced disproportionation[5-6] and so on.

The occurrence of hydrogen-induced disproportionation for  $ZrCo$  alloy is due to the intrinsic nature of this kind of alloy, namely formation of a more stable hydride  $ZrH_2$  and hydrogen non-absorptive metallic compound  $ZrCo_2$  other than typical hydride  $ZrCoH_3$  through hydrogen absorption by the alloy[7]. So when disproportionation reaction occurs,  $ZrCo$  alloy would lose its hydrogen isotope recovery and storage ability. Therefore, minimizing or addressing the disproportionation problem of  $ZrCo$  alloy is crucial.

Previous research has confirmed that disproportionation reaction would be effectively restrained if practical application temperature decreases below 623 K[8], namely the temperature in which equilibrium dissociation pressure of  $ZrCo$  alloy attains to 100 kPa. Therefore, a new  $ZrCo$  based hydride material that has lower dehydrogenation temperature than 623 K is needed.

Adding the third element is considered an effective way to elevate the equilibrium dissociation pressure and/or decrease the dehydrogenation temperature of  $ZrCo$  based hydrides, resulting in improving the anti-disproportionation property of  $ZrCo$  based alloy. Until now, there is little research reporting the addition

of the third element to this alloy except the Ref.[9]. The aim of the present paper is to synthesize  $Zr_{1-x}Hf_xCo$  and  $Zr_{1-x}Sc_xCo$  alloys that have a desirable isotherm with hydrogen, a higher dissociation pressure, a lower dehydrogenation temperature and other beneficial properties. And for this purpose Hf and Sc are selected as the third element because Hf or Sc can easily form a solid solution with Zr element and have high hydrogen storage capacity.

## 2 Experimental

$Zr_{1-x}Hf_xCo$  and  $Zr_{1-x}Sc_xCo$  ( $x=0, 0.1, 0.2$  and  $0.3$ , atom) alloys were prepared by magnetic levitation melting under an argon atmosphere. The purities of the raw material hafnium, scandium, zirconium and cobalt were above 99%. The ingots were turned over and remelted 3 times to ensure homogeneity.

The samples were crushed mechanically into powder in the air for hydrogen-absorption/dehydrogenation properties test. The alloy's crystal structures were studied by X-ray diffraction using Cu  $K\alpha$  radiation, 40 kV and 30 mA.

Pressure-composition-temperature(PCT) behaviors

of alloys were measured using a conventional volumetric method[8]. The temperature was controlled within  $\pm 1$  K during measurements.

## 3 Results and discussion

### 3.1 Performance of $Zr_{1-x}Hf_xCo$ alloy

Figs.1(a) and (b) show the XRD patterns for as-prepared and hydrided  $Zr_{1-x}Hf_xCo$  alloy, respectively. As seen in Fig.1(a), apparent single phases of cubic structures are observed, but it can not be concluded that the sample formed single solid solution, because a mixture of ZrCo and HfCo could show the similar pattern within the resolution limit; while in Fig.1(b), all patterns attribute to  $ZrCoH_3$  phase and no other peaks appear, indicating that  $Zr_{1-x}Hf_xCo$  alloy has good hydrogen stabilization.

Figs.2(a) and (b) show the dehydrogenation PCT curves for ZrCo alloy under different temperatures and  $Zr_{1-x}Hf_xCo$  alloy at 593 K, respectively. As seen in Fig.2(a), ZrCo alloy exhibits a single flat plateau in each dehydrogenation process, and with the increasing of temperature, its equilibrium dehydrogenation pressure increases but the corresponding plateau region's width

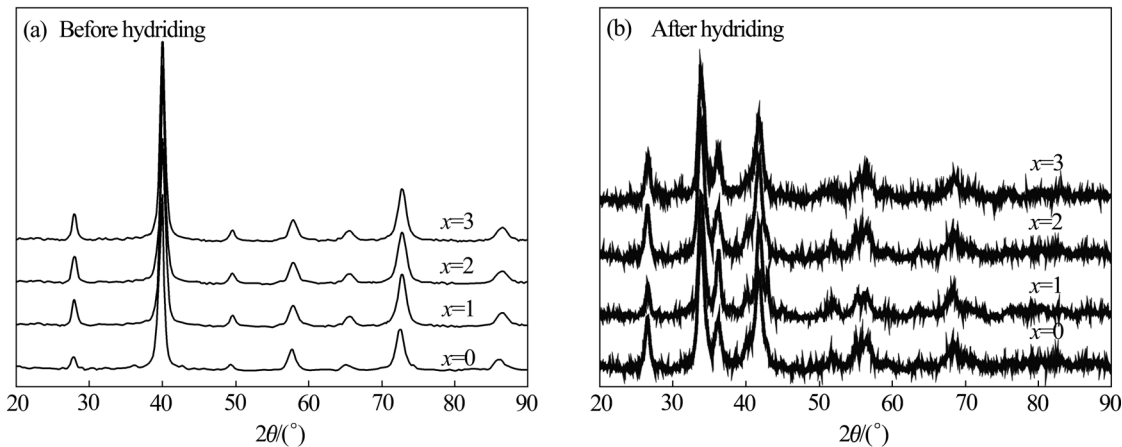


Fig.1 XRD patterns for as-prepared  $Zr_{1-x}Hf_xCo$  (a) and after hydrogen absorbed  $Zr_{1-x}HfCo$  (b)

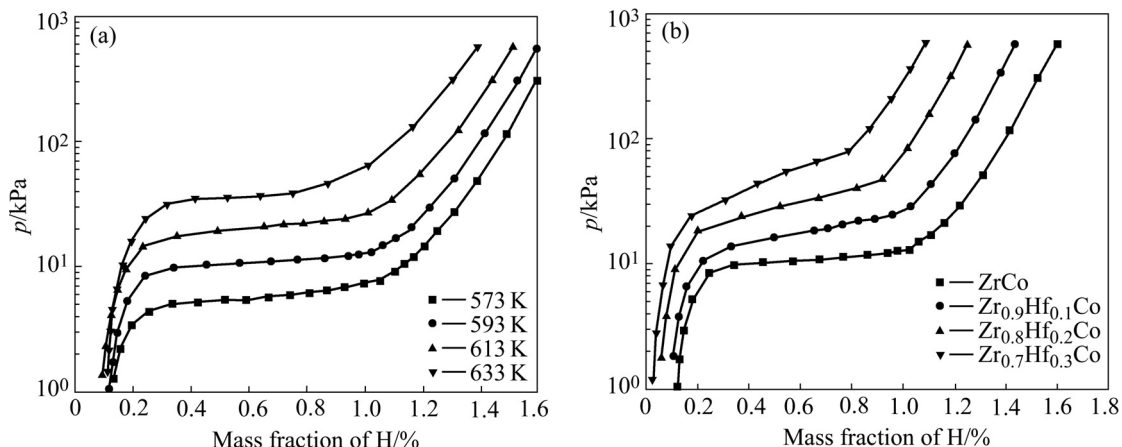


Fig.2 Dehydrogenation PCT curves for ZrCo alloy under different temperatures (a) and  $Zr_{1-x}Hf_xCo$  ( $x=0, 0.1, 0.2, 0.3$ ) (b) at 593 K

decreases; Fig.2(b) shows, with increasing Hf content, the equilibrium dehydrogenation pressure of  $Zr_{1-x}Hf_xCo$  alloy is elevated to a higher value, but the plateau region's width is further shortened and slope of plateau region gets steeper. Combined with XRD patterns of  $Zr_{1-x}Hf_xCo$  alloy shown in Fig.1(a) and the fact of that the HfCo alloy has much higher equilibrium dehydrogenation pressure than ZrCo alloys do, the single dehydrogenation plateau of each isotherm in Fig.2(b) indicates that the synthesized material of composition  $Zr_{1-x}Hf_xCo$  forms a single solid solution other than a mixture of the alloys ZrCo and HfCo. In the repeated hydrogenation-dehydrogenation cycles, no change in this feature has been observed, indicating that these solid solutions are rather stable under the experimental conditions.

The temperature dependence of the equilibrium dehydrogenation pressure for  $Zr_{1-x}Hf_xCo$  alloy is plotted in Van't Hoff form as Fig.3, where linear relations are observed for all these alloys, and one can see that at the same isothermal temperature the equilibrium dehydrogenation pressure of  $Zr_{1-x}Hf_xCo$  alloy increases with the sequence of  $ZrCo < Zr_{0.9}Hf_{0.1}Co < Zr_{0.8}Hf_{0.2}Co < Zr_{0.7}Hf_{0.3}Co$ .

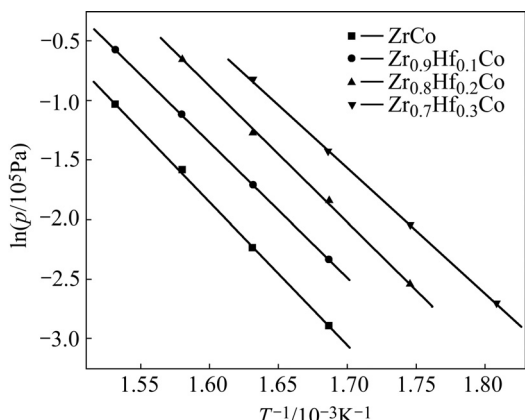


Fig.3 Van't Hoff curves for  $Zr_{1-x}Hf_xCo$  alloy

Table 1 lists the dehydrogenation enthalpy and entropy values of  $Zr_{1-x}Hf_xCo$  alloy calculated according to their Van't Hoff equations. With increasing Hf substitution content,  $\Delta H$  decreases gradually and  $\Delta S$  changes little. In terms of thermodynamics, we know that as dehydrogenation  $\Delta H$  value of hydrided  $Zr_{1-x}Hf_xCo$  gets less, it becomes easier for them to release hydrogen, appearing as isotherm plateau pressure elevated to a higher value at the same dehydrogenation temperature with increasing Hf substitution content, which is coincident with Fig.1(b).

Fig.4 shows the changing curves of  $Zr_{1-x}Hf_xCo$  alloys for both the dehydrogenation temperatures for supplying 100 kPa hydrogen and maximum hydrogen storage capacity at room temperature vs Hf substitution

Table 1 Dehydrogenation  $\Delta H$  and  $\Delta S$  for  $Zr_{1-x}Hf_xCo$  alloy

Alloy	$\Delta H/(kJ \cdot mol^{-1})$	$\Delta S/(J \cdot mol^{-1} \cdot K^{-1})$
ZrCo	-97.8	145.5
$Zr_{0.9}Hf_{0.1}Co$	-92.3	140.2
$Zr_{0.8}Hf_{0.2}Co$	-90.8	141.9
$Zr_{0.7}Hf_{0.3}Co$	-87.0	141.0

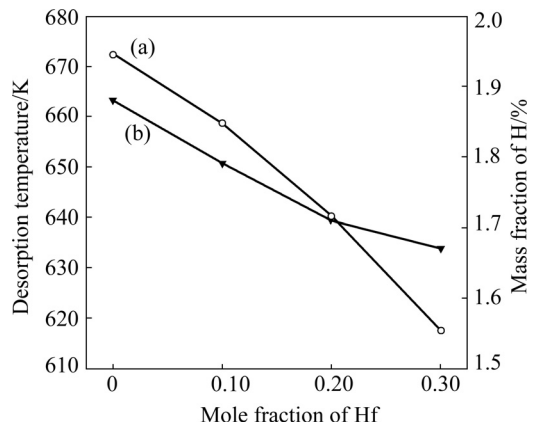


Fig.4 Curves of  $Zr_{1-x}Hf_xCo$  alloy for dehydrogenation temperatures for supply 100 kPa hydrogen (a) and maximum hydrogen storage capacity at room temperature (b)

content. It can be seen from the curve (a) in Fig.4 that the dehydrogenation temperatures for supplying 100 kPa hydrogen decrease with increasing Hf substitution content, which are about 672, 658, 640 and 617 K for ZrCo,  $Zr_{0.9}Hf_{0.1}Co$ ,  $Zr_{0.8}Hf_{0.2}Co$  and  $Zr_{0.7}Hf_{0.3}Co$  alloy, respectively. However, the maximum hydrogen storage capacity of  $Zr_{1-x}Hf_xCo$  alloy at room temperature reduces with increasing Hf content slightly, which are about 1.88, 1.79, 1.71 and 1.67% (mass fraction), respectively, as shown in the curve (b) of Fig.4.

The increase of equilibrium dehydrogenation pressure of  $Zr_{1-x}Hf_xCo$  alloy can be interpreted by the denser electron concentration through substitution of Hf for Zr. Since the atomic number of Hf is greater than that of Zr by 32 and they have almost identical atomic radius, the outer electron concentration of Hf is much denser than Zr. The increase of electron concentration makes deposit of hydrogen atom in alloy cavity unstable, resulting in the increase of equilibrium dehydrogenation pressure of  $Zr_{1-x}Hf_xCo$  alloy with increasing Hf substitution content.

### 3.2 Performance of $Zr_{1-x}Sc_xCo$ alloy

Figs.5(a) and (b) show the XRD patterns for as-prepared and hydrided  $Zr_{1-x}Sc_xCo$  alloy, respectively. Just like  $Zr_{1-x}Hf_xCo$  alloy shown in Fig.1, the as-prepared and hydrided  $Zr_{1-x}Sc_xCo$  alloys show the patterns of ZrCo and  $ZrCoH_3$  phase, respectively. This indicates that the synthesized material of composition  $Zr_{1-x}Sc_xCo$  forms a single solid solution as well.

Figs.6(a) and (b) show the dehydrogenation PCT

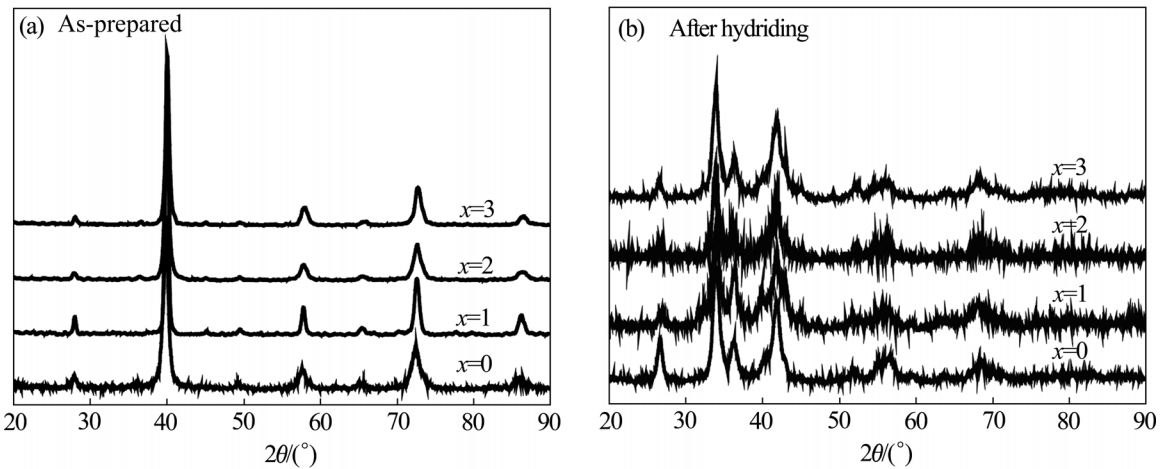


**Fig.5** XRD patterns for of  $Zr_{1-x}Sc_xCo$  as-prepared (a) and after hydrogen absorption (b) at room temperature

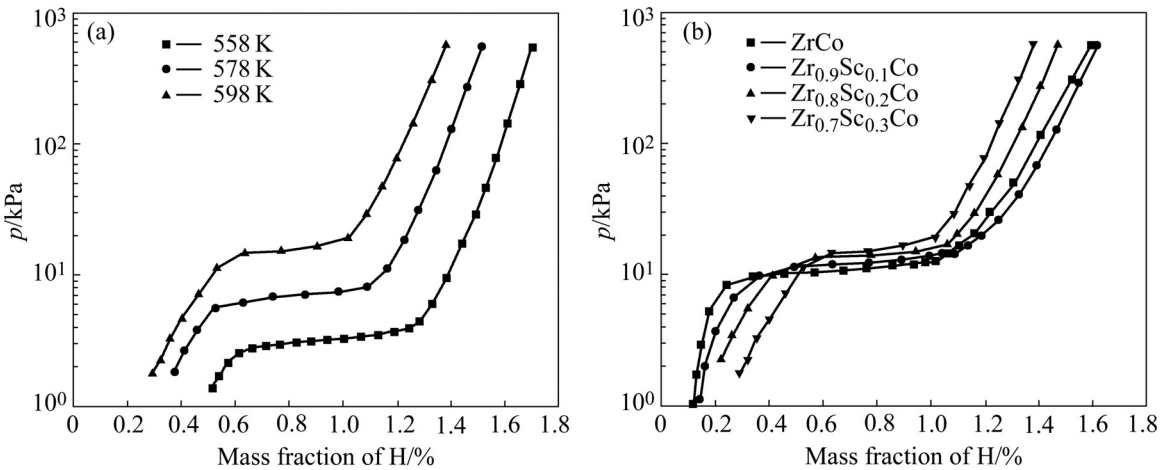


**Fig.6** Dehydrogenation PCT curves for  $Zr_{0.7}Sc_{0.3}Co$  alloy under different temperatures (a) and  $Zr_{1-x}Sc_xCo$  ( $x=0, 0.1, 0.2, 0.3$ ) at 593 K (b)

curves for  $Zr_{0.7}Sc_{0.3}Co$  alloy under three different temperatures and  $Zr_{1-x}Sc_xCo$  alloy at 593 K, respectively. As seen in Fig.6(a),  $Zr_{0.7}Sc_{0.3}Co$  alloy exhibits a single flat plateau in each dehydrogenation process just like ZrCo alloy, but with increasing dehydrogenation temperature, its corresponding plateau region's width decreases seriously. As seen in Fig.6(b), with increasing Sc content, the equilibrium dehydrogenation pressure of  $Zr_{1-x}Sc_xCo$  alloy is heightened little, but the plateau region's width is greatly shortened, which is a big disadvantage for dehydrogenation property of  $Zr_{1-x}Sc_xCo$  alloy.

Fig.7 shows Van't Hoff curves for  $Zr_{1-x}Sc_xCo$  alloy. Linear relations are observed for all these alloys as well. It can be seen that at the same isotherm temperature under the experimental conditions, the equilibrium dehydrogenation pressure of  $Zr_{1-x}Sc_xCo$  alloy increases with the sequence of  $ZrCo < Zr_{0.9}Sc_{0.1}Co < Zr_{0.8}Sc_{0.2}Co < Zr_{0.7}Sc_{0.3}Co$ , but the difference among them is quite

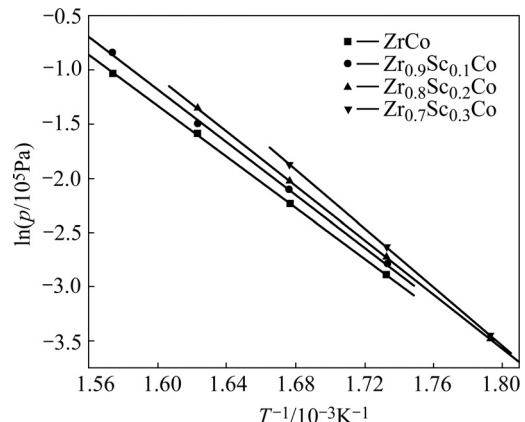


**Fig.7** Van't Hoff curves for  $Zr_{1-x}Sc_xCo$  alloy

small.

Table 2 shows the dehydrogenation enthalpy and entropy values of  $Zr_{1-x}Sc_xCo$  alloy. With increasing Sc substitution content, both  $\Delta H$  and  $\Delta S$  increase gradually. The increase of dehydrogenation  $\Delta H$  values of hydrided

$Zr_{1-x}Sc_xCo$  means that with increasing Sc substitution content, it becomes more difficult to release hydrogen, which is coincident with the fact of that effective dehydrogenation capacity decreases greatly with the increasing of Sc content while the dehydrogenation pressure is almost the same at the same isotherm temperature shown in Fig.6.

**Table 2** Dehydrogenation  $\Delta H$  and  $\Delta S$  for  $Zr_{1-x}Sc_xCo$  alloy

Alloy	$\Delta H/(kJ \cdot mol^{-1})$	$\Delta S/(J \cdot mol^{-1} \cdot K^{-1})$
ZrCo	-97.8	145.5
$Zr_{0.9}Sc_{0.1}Co$	-102.8	154.8
$Zr_{0.8}Sc_{0.2}Co$	-110.0	170.2
$Zr_{0.7}Sc_{0.3}Co$	-112.1	172.5

Fig.8 shows the changing curves of  $Zr_{1-x}Sc_xCo$  alloy of both dehydrogenation temperature for supplying 100 kPa hydrogen and maximum hydrogen storage capacity at room temperature versus Sc content. The dehydrogenation temperature for supplying 100 kPa hydrogen decreases slightly with the increasing of Sc substitution content, which are about 672, 664, 652 and 650 K for the ZrCo,  $Zr_{0.9}Sc_{0.1}Co$ ,  $Zr_{0.8}Sc_{0.2}Co$  and  $Zr_{0.7}Sc_{0.3}Co$  alloy, respectively, and the maximum hydrogen storage capacity of  $Zr_{1-x}Sc_xCo$  alloy at room temperature increases with increasing Sc content, which are about 1.88, 1.95, 2.03 and 2.08% (mass fraction), respectively.

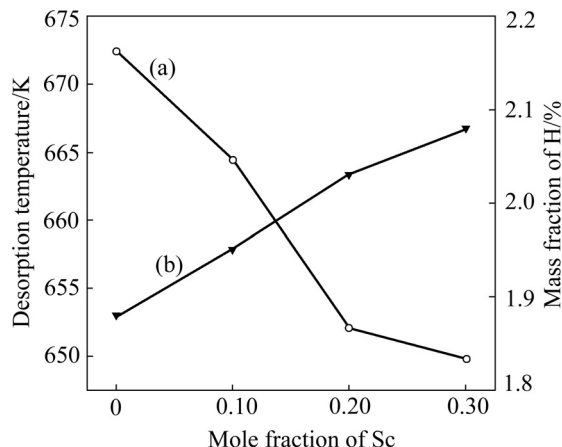


**Fig.8** Curves of  $Zr_{1-x}Sc_xCo$  alloy of dehydrogenation temperatures for supply 100 kPa hydrogen (a) and maximum hydrogen storage capacity (b) at room temperature

#### 4 Conclusions

To lower dehydrogenation temperature of ZrCo alloy for supplying 100 kPa hydrogen to address its

disproportionation, Hf and Sc are selected to substitute Zr partly to develop metallic compounds for tritium recovery, storage and supply.

1) Both as-prepared  $Zr_{1-x}M_xCo$  ( $M=Hf, Sc; x=0, 0.1, 0.2, 0.3$ ) and hydrogen absorbed  $Zr_{1-x}Sc_xCo$  ( $x=0, 0.1, 0.2, 0.3$ ) alloy form stable single solid solution identical with ZrCo and hydride similar to  $ZrCoH_3$  after hydrogen absorption.

2) Each of these alloys has high hydrogen storage capacity. However, substitution of Hf for Zr obviously elevates the equilibrium dehydrogenation pressure of ZrCo alloy, while substitution of Sc for Zr makes its dehydrogenation more difficult. When Hf substitution content reaches 30% (mole fraction), dehydrogenation temperature for supplying 100 kPa hydrogen for  $Zr_{0.7}Hf_{0.3}Co$  alloy decreases to below 623 K, namely 617 K.

3) The thermodynamic calculation of these alloys shows that  $\Delta H$  of  $Zr_{1-x}Hf_xCo$  alloy decreases with increasing Hf substitution content, while  $Zr_{1-x}Sc_xCo$  alloy behaves oppositely, which is coincident with their dehydrogenation property.

#### References

- [1] SHMAYDA W T, HEICS A G, KHERANI N P. Comparison of uranium and zirconium cobalt for tritium storage [J]. Journal of the Less-Common Metals, 1990, 162(1): 117–127.
- [2] KONISHI S, NAGASAKI T, YOKOKAWA N, NARUSE Y. Development of zirconium-cobalt beds for recovery, storage and supply of tritium [J]. Fusion Engineering and Design, 1989, 10: 355–358.
- [3] PENZHORN R D, DEVILLERS M, SIRCH M. Evaluation of ZrCo and other getters for tritium handling and storage [J]. Journal of Nuclear Materials, 1990, 170(3): 217–231.
- [4] NAIK Y, RAMA RAO G A, VENUGOPAL V. Zirconium-cobalt intermetallic compound for storage and recovery of hydrogen isotopes [J]. Intermetallics, 2001, 9(4): 309–312.
- [5] HARA M, OKABE T, MORI K, WATANABE K. Kinetics and mechanism of hydrogen-induced disproportionation of ZrCo [J]. Fusion Engineering and Design, 2000, 49/50: 831–838.
- [6] KONISHI S, NAGASAKI T, OKUNO K. Reversible disproportionation of ZrCo under high temperature and hydrogen pressure [J]. Journal of Nuclear Materials, 1995, 223(3): 294–299.
- [7] BEKRIS N, BESSERER U, SIRCH M, PENZHORN R D. On the thermal stability of the zirconium/cobalt-hydrogen [J]. Fusion Engineering and Design, 2000, 49/50: 781–789.
- [8] HARA M, HAYAKAWA R, KANEKO Y, WATANABE K. Hydrogen-induced disproportionation of  $Zr_2M$  ( $M=Fe, Co, Ni$ ) and reproporation [J]. Journal of Alloys and Compounds, 2003, 352(1/2): 218–225.
- [9] KONISHI S, NAGASAKI T, HAYASHI T, OKUNO K. Equilibrium hydrogen pressure on the solid solutions of ZrCo-HfCo intermetallic compounds [J]. Journal of Nuclear Materials, 1995, 223(3): 300–304.

(Edited by LAI Hai-hui)